SOLITON PHASE SHIFTS IN A DISSIPATIVE LATTICE

Nayeem Islam

Kenneth Steiglitz

CS-TR-044-86

June 1986

Soliton Phase Shifts in a Dissipative Lattice†

Nayeem Islam and Kenneth Steiglitz
Dept. of Computer Science
Princeton University
Princeton, NJ 08544

Abstract

We report measurements of soliton phase shifts resulting from head-on collisions in the *LC* lattice of Hirota and Suzuki, the electrical analog of the Toda Lattice. The effect of dissipation along this lattice is to decrease the amplitude and increase the width of the solitons as they travel down the lattice. To within experimental error, however, we found that the velocity and phase shifts remain constant, so that a soliton species is uniquely determined by its velocity. This shows that the positional phase of such solitons can be used to encode information in a very simple way, and that the lattice can be used to do computation, of which parity checking is a simple example.

1. Introduction

Hirota and Suzuki [1] built a network consisting of a ladder of inductors and nonlinear capacitors. This non-linear network supports solitons, and is the electrical analog of the mechanical lattice analyzed by Toda [2], which is made of balls of unit mass connected by nonlinear springs. These masses interact with their nearest neighbors via an exponential potential. The equation governing the generalized momentum of a unit mass in this system is equivalent to the equation governing the voltage at a point on the lattice. In the continuum limit both equations reduce to the K-dV equation [2].

In [3,6] it is suggested that if the positional phase of a soliton is used to encode information, the phase shifts resulting from collisions can accomplish useful computation. This idea springs from work with cellular automata that support soliton-like structures, and the design of a carry-ripple adder using these "pseudo-solitons" is described in [6]. To carry this idea over to solitons supported by physical systems, however, it is important that the phase shifts on collisions depend only on the species of soliton, and not on the position where the collision takes place.

The experiment reported here, then, was motivated by this question of whether the soliton phase shifts in the Hirota-Suzuki lattice are determined only

† This work was supported by NSF Grant ECS-8414674 and U. S. Army Research-Durham Contract DAAG29-85-K-0191.

by the identity of the solitons. We recreated a lattice similar to that described by Hirota and Suzuki and measured phase changes that result from the head-on collision between two solitons moving in opposite directions. The Appendix contains a description of our apparatus and the procedures. The results reported by Hirota and Suzuki do not show the effects of dissipation in the lattice, but in our implementation these effects are appreciable.

In the dissipationless lattice, the amplitude, velocity, width, and phase changes between colliding solitons are all closely related, but once determined remain invariant with respect to position along the lattice. With dissipation, however, the soliton amplitude decreases as it travels along the lattice, with a corresponding increase in width. However, we found that the velocity remains constant — and therefore that the species, or identity, of a soliton is uniquely determined by its velocity. Moreover we found that the phase change resulting from a collision is dependent only on the species of solitons involved, and not on the particular amplitudes and widths at the moment of collision. We also observed some effects reported by Hammack and Segur [9] in their experiments on dissipative water waves.

Finally, we will discuss the possible computational uses of solitons. The results allow us to encode a bit in the positional phase of a soliton in a natural way, and we are able to construct a very simple parity-checker with the lattice.

2. Velocity and Amplitude Measurements

There are 80 sections in the lattice and the physical circuit would measure about 2 meters if fully extended. Figure 1 shows the measured amplitude of a typical soliton with respect to distance along the lattice, in logarithmic units. The decrease in the amplitude of solitons was approximately exponential. This can be attributed to two factors:

1) There is Ohmic dissipation in the windings of the coils and the interconnection wires;
2) The small oscillatory tail that follows the passage of a soliton can briefly forward bias the varactor diodes, causing them to conduct current.

Variation of dissipation coeff. with reverse bias	
reverse bias(V)	dissipation coeff
-0.12	-0.001201
-0.20	-0.001210
-0.28	-0.001337
-0.36	-0.001878
-0.42	-0.002753
-0.50	-0.002948

Table 1

The dissipation was dependent on both initial amplitude and on the reverse bias on the varactor diodes. The greater the initial amplitude or the reverse bias the greater the dissipation. Figure 2 shows the variation of soliton amplitude with lattice position for various reverse biases, while Table 1 gives the corresponding variation in the estimated exponent γ in the relation

$$A(n) = A_1 e^{\gamma n}$$

where A(n) is the amplitude at Lattice Position n, and A_1 is the amplitude at Lattice Position 1. The values of γ were obtained by a least-squares regression on the log-amplitude data. Figure 3 and Table 2 show the corresponding information for various initial amplitudes. These results can be explained by the fact that the higher the reverse bias or initial amplitude the closer the diodes are to their break voltage, making it easier for a soliton to forward bias them. Thus, the exponent γ becomes more negative with higher reverse bias and initial amplitude. We would expect the effect of Ohmic dissipation to stay constant.

Variation of dissipation coeff. with initial amplitude	
init. amp.	dissipation coeff
2	-0.001480
3	-0.001492
4	-0.001450
5	-0.001661
6	-0.002116

Table 2

In the dissipative system described by Hammack and Segur [9], the water level around the soliton increases as it loses amplitude. A similar affect was noticed in our lattice — as a soliton loses amplitude the reverse bias increases. The explanation offered by Hammack and Segur [9] is that as the solitons lose energy due to viscous affects, the total mass of the waves is conserved. Thus, as mass gets forced out of the solitons, it raises the average water level behind them. In our system charge is similarly conserved, and as the soliton loses charge it goes into increasing the forward bias of the varactor diodes. This increase in water level is referred to as a "shelf" in [5, p. 284].

Even though the amplitude of a soliton decreases down the lattice, its velocity was observed to stay constant to within a few percent. Figure 4 shows a typical plot of delay time vs. lattice position, showing this linear relationship. The same linear relationship was observed for various initial amplitudes and reverse biases. For each particular velocity there is an amplitude-width curve (see Fig. 5), and the curves for different velocities do not overlap with each other.

A soliton forms in the first few lattice sections, and its velocity in this formation zone is lower than in the rest of the lattice. The effect of this formation zone was also evident in the regression analyses of amplitude vs. reverse bias and amplitude vs. initial bias. In both regressions, the fit after the fifth section was much better than at earlier points, and the first two data points were always anomalous. A soliton thus stabilizes its behavior only after passing through this formation zone. We might also mention that the variation of amplitude with lattice position is not quite exponential: Close inspection of the log-amplitude vs. position curve in Fig. 1 shows that there is a knee at about the 40th lattice section, at which point the slope decreases.

3. Phase Shifts on Collision

We now come to the main point of our experiments — the measurement of phase shifts resulting from head-on collisions between two solitons. Our results show that these phase shifts depend only on the velocities of the two colliding solitons, and is not affected by the decrease in amplitude once the solitons are formed. This was tested by holding the initial pulse amplitudes constant and varying the location of collision in the lattice. The variation of amplitude with position means that the pair of amplitude values at each point in the lattice is different. Figure 6 shows the relationship between phase shift and location of collision for a typical case. The phase shifts are constant to within 3%.

Maxworthy [8] measured positional phase shifts resulting from head-on collisions (using reflection) between two water waves of equal initial amplitudes, and found them independent of those initial amplitudes. Our main experiment and result, showing that phase shift is independent of the variations in amplitude and width due to dissipation, is therefore quite different. We did repeat Maxworthy's experiment, varying the initial amplitudes, and hence the velocities, and found the dependence of phase change on velocity shown in Fig. 7. Our results indicate that the phase shift increases with increasing velocity, and with increasing initial amplitude, and are thus closer to the theoretical predictions described by Maxworthy [9] than his own experimental results.

4. A Design for a Parity Checker

The phase changes can be exploited to design a parity checker. The scheme will depend heavily on the fact that a phase change is independent of where the collision takes place on the lattice once the initial amplitude is set. For safety all collisions are forced into the region where the phase position relationship is known (see Fig. 6).

The idea is simple. We send a "parity-checker" soliton down one end of the lattice, and send the data bits encoded in solitons from the other end. The phase of the parity checker soliton when it arrives at the other end of the lattice will indicate whether or not the parity of the data bits is odd or even.

For encoding purposes the following method is used. A '0' bit is represented by one soliton and a '1' by two solitons, so that if collision with a '0' causes a phase change of x in the checker soliton, collision with a '1' causes a phase change of $2x$. After the checker soliton passes through all the data solitons, its phase mod(x) will be 0 or 1, if the data stream had an even or odd number of 0's, respectively.

To see how this would work in practice, we generated pulses for a 3-bit data stream, using wave function generators in burst mode, where one can be triggered by the other. The settings on the two function generators were:

1) repetition rate: 1.07 kHz, initial pulsewidth: 194 ns, initial amplitude: 3.3 V, Offset: -0.28 V.

2) repetition rate: 871 kHz, initial pulsewidth: 287 ns, initial amplitude: 2.11 V, Offset: -0.28 V.

Phase shifts that can be used in a 3-bit parity checker	
Collision #	Phase shift(μs)
1	0.134
2	0.132
3	0.136
4	0.134
5	0.138
6	0.138

Table 3

Table 3 gives the measured phase shifts associated six consecutive collisions. The parity-checker soliton will appear at the end of the lattice delayed by a multiple of the average delay, 0.1353 μs. In our setup the normal undeflected delay was 13.415 μs.

To decode the answer, the output checker soliton can be amplified (so that it can drive a logic gate), and then ANDed with a 7.3892 MHz clock. The checker soliton will survive the AND operation if and only if it undergoes an even number of collisions. Note that the smallest and largest phase changes above will not cause detection problems if the solitons are sharp enough pulses.

The oscillatory tails that often follow solitons tended to degrade the soliton waveforms. This effect can be reduced by using wider input pulses. However, the pulse width must stay below the transition value, the value where the initial pulse produces two solitons instead of one. We found this to be about 300 ns for our initial conditions.

5. Summary

Our results suggest that in the Hirota-Suzuki lattice the properties of a soliton are fixed once it is introduced into the lattice, and are not affected by the decrease in amplitude caused by dissipation. We found that even when the amplitudes decreased by a factor of two, there was no significant change in velocity or in the phase change that results from collisions. The independence of velocity on amplitude is similar to the behavior of solitons in the non-linear Schrödinger equation with dissipation [5, pp. 270-271]. Theoretical or computational verification of our results requires further work on the Lattice model with dissipation.

We described a simple parity checker based on the idea that information can be encoded in the phase of a soliton. It will be interesting to see if more sophisticated computation can be implemented this way. Fiber optical transmission lines, which support envelope solitons, are fast and small enough to offer an attractive medium for such an application.

REFERENCES

1. R. Hirota and K. Suzuki, "Theoretical and experimental studies of Lattice Solitons in Nonlinear Lumped Networks," *Proc. IEEE*, vol. 61, pp. 1483-1492, Oct. 1973.
2. M. Toda, "Waves in Nonlinear Lattices," *Prog. Theor. Phys. Suppl.*, vol. 45, pp. 174-200, 1970.
3. J. K. Park, K. Steiglitz, W. P. Thurston, "Soliton-like Behavior in Automata" *Physica D*, vol. 19D, pp. 23-32, 1986.
4. J. P. Leane, "Solitons and Nonlinear Wave Motion," Senior Thesis, Dept. of Physics, Princeton University, 1984.
5. M. J. Ablowitz, H. Segur, *Solitons and the Inverse Scattering Transform,* SIAM, Philadelphia, 1981.
6. K. Steiglitz, Kamal I., Watson A., "Embedding Computation in One-Dimensional Automata by Phase-Coding Solitons," Tech. Rep. 15, Dept. of Computer Science, Princeton University, Nov. 1985.
7. A. Bar-Lev, *Semiconductors in Electronic Devices,* Prentice-Hall, London, 1979.
8. T. Maxworthy, "Experiments on Collisions between Solitary Waves," *J. Fluid Mech.*, vol. 76, (1976).
9. J. L. Hammack, H. Segur "The Kortweg-de Vries Equation and Water Waves: Part 2. Comparison with Experiments," *J. Fluid Mech*, vol. 65, pp. 289-314, 1974.

APPENDIX

Experimental Details

The Hirota-Suzuki nonlinear LC lattice used in these experiments is low-pass in the small-signal limit; that is, the inductors are in the series arms and the capacitors in the parallel arms. Altogether there were 80 four-terminal sections, each consisting of an inductor and capacitor. We used reversed-biased varactor diodes (Phillips ECG 618) for the voltage-dependent capacitors, and ferrite-core coils (J. W. Miller Part No. 4628) with a nominal inductance of 39μH for the linear inductances. The diodes had a measured capacitance of 440 pF at 1.2V and a minimum Q of 200 at 1V.

Solitons are observed by applying to one end of the lattice a pulse with amplitude between 1V and 6V with a DC bias between -0.2V and -0.5V. We attempted to terminate the other end of the lattice with a characteristic impedance, which, because the circuit is nonlinear, varies with frequency. In our experiments the repetition rate of the pulses was used to calculate the termination impedance, and this value was fine-tuned experimentally to prevent reflection. The output impedance of the function generator was very high, and therefore required an operational amplifier to isolate it and make its effective impedance low.

The voltage dependence of the capacitor that is required by the Toda model is logarithmic:

$$C(V) = C_0(\frac{V_0}{V}) \ln(1 + \frac{V}{V_0}) \tag{1}$$

The Taylor series expansion of this is

$$C_0[1 - \frac{1}{2}\frac{V}{V_0} + \frac{1}{3}(\frac{V}{V_0})^2 - \frac{1}{4}(\frac{V}{V_0})^3 \cdots] \tag{2}$$

The actual variation of the capacitance is shown in Fig. 8, and is predicted by theory to be of the form [7, pp. 131-134]

$$C(V) = \frac{\overline{C}_0}{[1 + \frac{V}{\phi_0}]^2} \tag{3}$$

We measured $\phi_0 = -0.64\,V$, and obtained the value $\overline{C}_0 = 780$ pF from the graph. Equation (3) has the Taylor series expansion

$$\overline{C}_0\ [1 - 2\frac{V}{\phi_0} + 3(\frac{V}{\phi_0})^2 - 4(\frac{V}{\phi_0})^3 \cdots] \tag{4}$$

Choosing $C_0 = \overline{C}_0$ and $V_0 = \phi_0/4$ in (4) yields

$$C_0 \left[1 - \frac{1}{2}\frac{V}{V_0} + \frac{3}{16}\left(\frac{V}{V_0}\right)^2 - \frac{1}{16}\left(\frac{V}{V_0}\right)^3 \cdots \right] \tag{5}$$

which agrees with (2) to first order. We note that Leane [4] claims that many nonlinear functions besides the logarithm also produce solitons.

Figure Captions

Fig. 1 Measured logarithm of the amplitude in volts of a typical soliton vs. distance along the lattice. Initial amplitude = 4 V; DC bias = -0.27 V; initial pulse width = 90 ns, repetition rate = 2 kHz.

Fig. 2 Amplitude of typical solitons vs. position for various reverse biases. Initial amplitude = 1.72 V; DC bias = -0.12 V to -0.5 V; initial pulse width = 279 ns, repetition rate = 1.09 kHz.

Fig. 3 Amplitude of typical solitons vs. position for various initial amplitudes. Initial amplitude = 2.0 V to 6.0 V; DC bias = -0.32 V; initial pulse width = 200 ns; repetition rate = 5.0 kHz.

Fig. 4 Delay time of a typical soliton vs. lattice position. Initial amplitude = 4.4 V; DC bias = -0.27 V; initial pulse width = 217 ns; repetition rate = 1.09 kHz.

Fig. 5 Amplitude vs. width for solitons of various velocities. Initial amplitude = 2.0 V to 5.0 V; DC bias = -0.31 V; initial pulse width = 114 ns; repetition rate = 5.0 kHz.

Fig. 6 Phase shift vs. location of collision for a pair of typical solitons. First function generator: Initial amplitude = 3.29 V; DC bias = -0.28 V; initial pulse width = 194 ns; repetition rate = 1.09 kHz. Second function generator: Initial amplitude = 2.11 V; DC bias = -0.28 V; initial pulse width = 286 ns; repetition rate = 252 kHz.

Fig. 7 Phase shift vs. velocity for head-on collisions of solitons with equal initial amplitudes. First function generator: Initial amplitude = 1.5 V to 4.5 V; DC bias = -0.28 V; initial pulse width = 160 ns; repetition rate = 1.17 kHz. Second function generator: Initial amplitude = 1.5 V to 4.5 V; DC bias = -0.28 V; initial pulse width = 160 ns; repetition rate = 5.19 kHz.

Fig. 8 Measured C-V plot for varactor diode; only negative voltages, corresponding to reverse biases, are of interest.

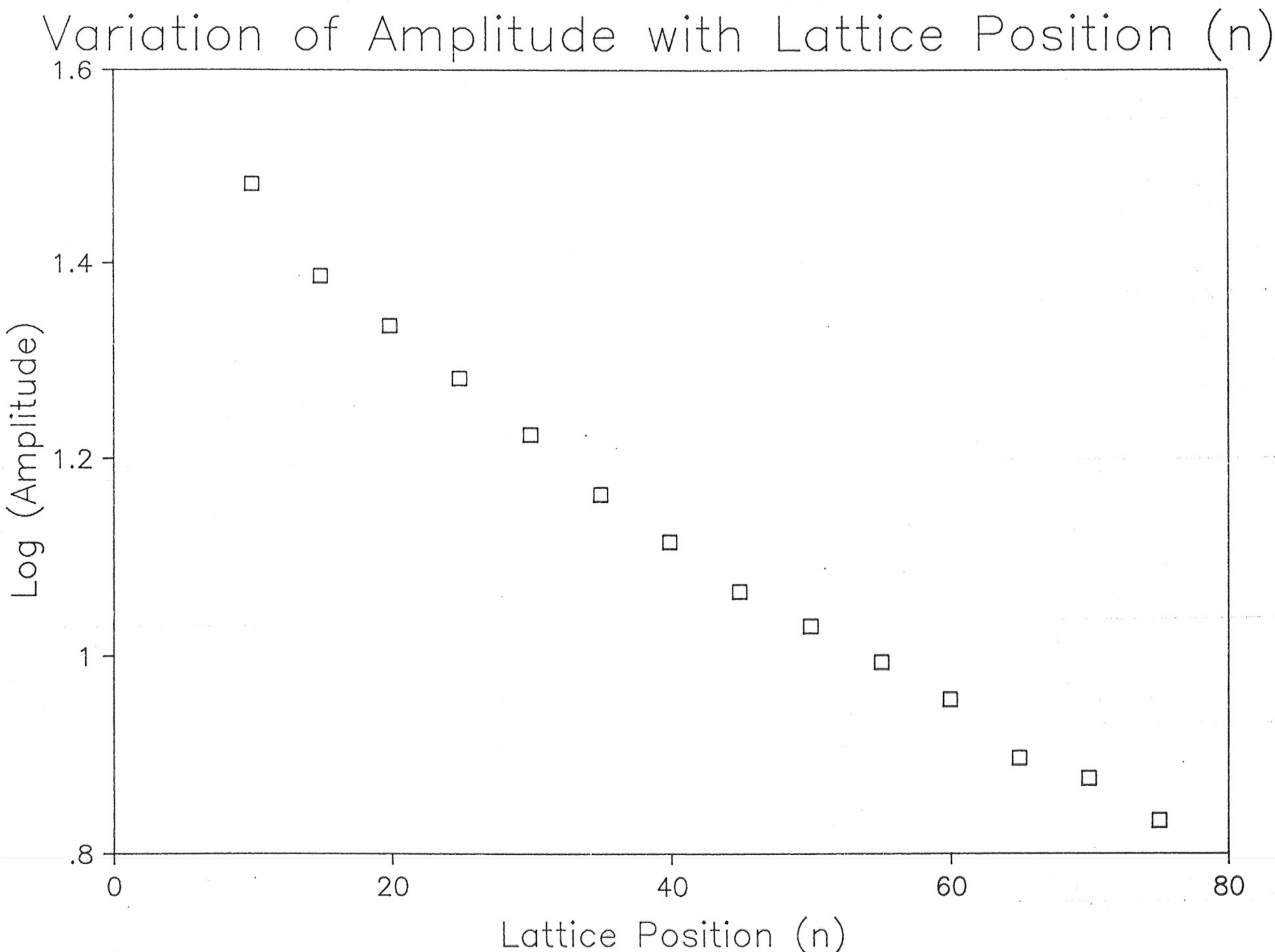
Variation of Amplitude with Lattice Position (n)
1.6
1.4
1.2
1
.8
Log (Amplitude)
0
20
40
60
80
Lattice Position (n)

Figure 1

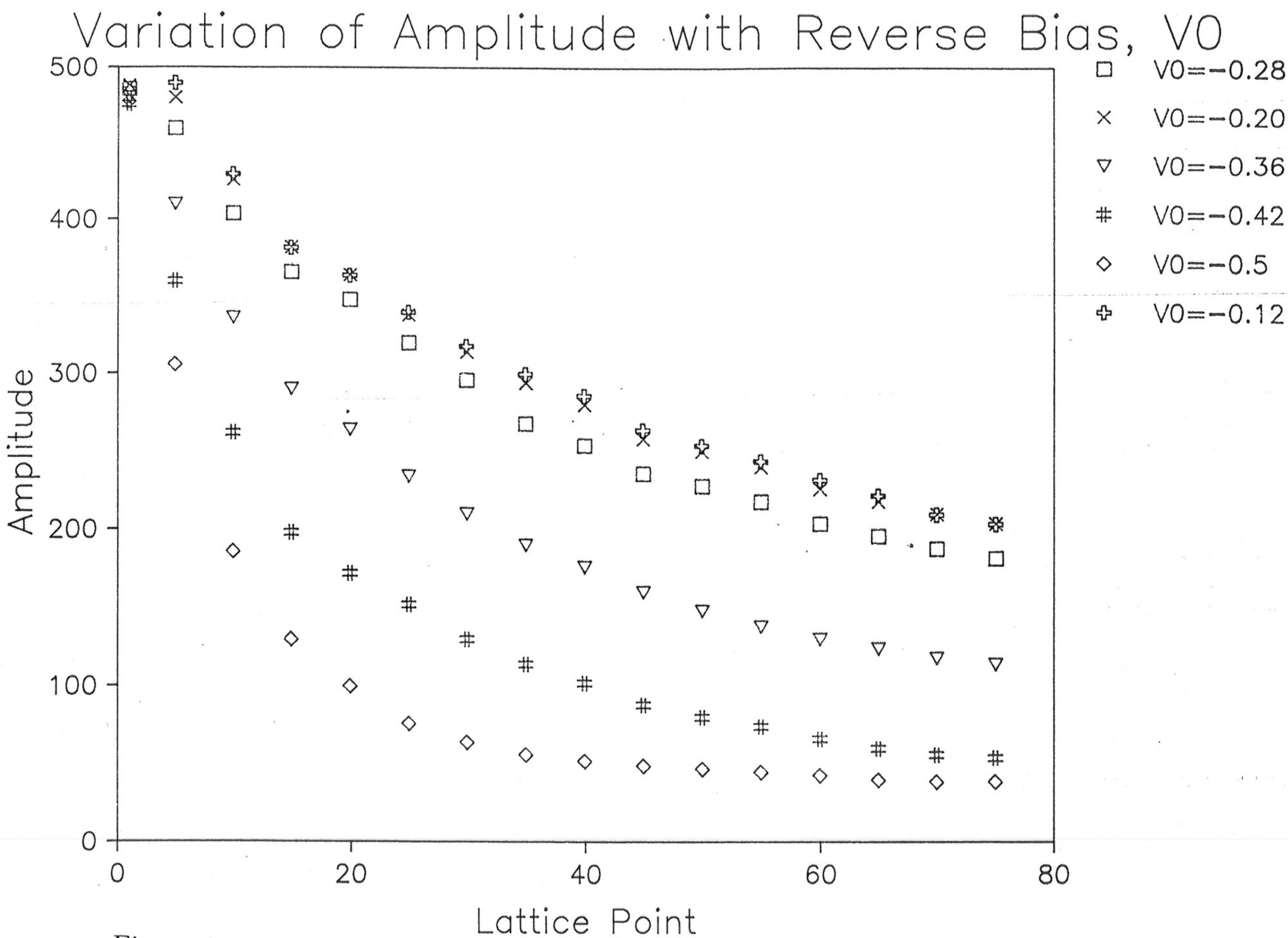

Variation of Amplitude with Reverse Bias, V0
Amplitude
Lattice Point
V0=−0.28
V0=−0.20
V0=−0.36
V0=−0.42
V0=−0.5
V0=−0.12
500
400
300
200
100
0
0
20
40
60
80

Figure 2

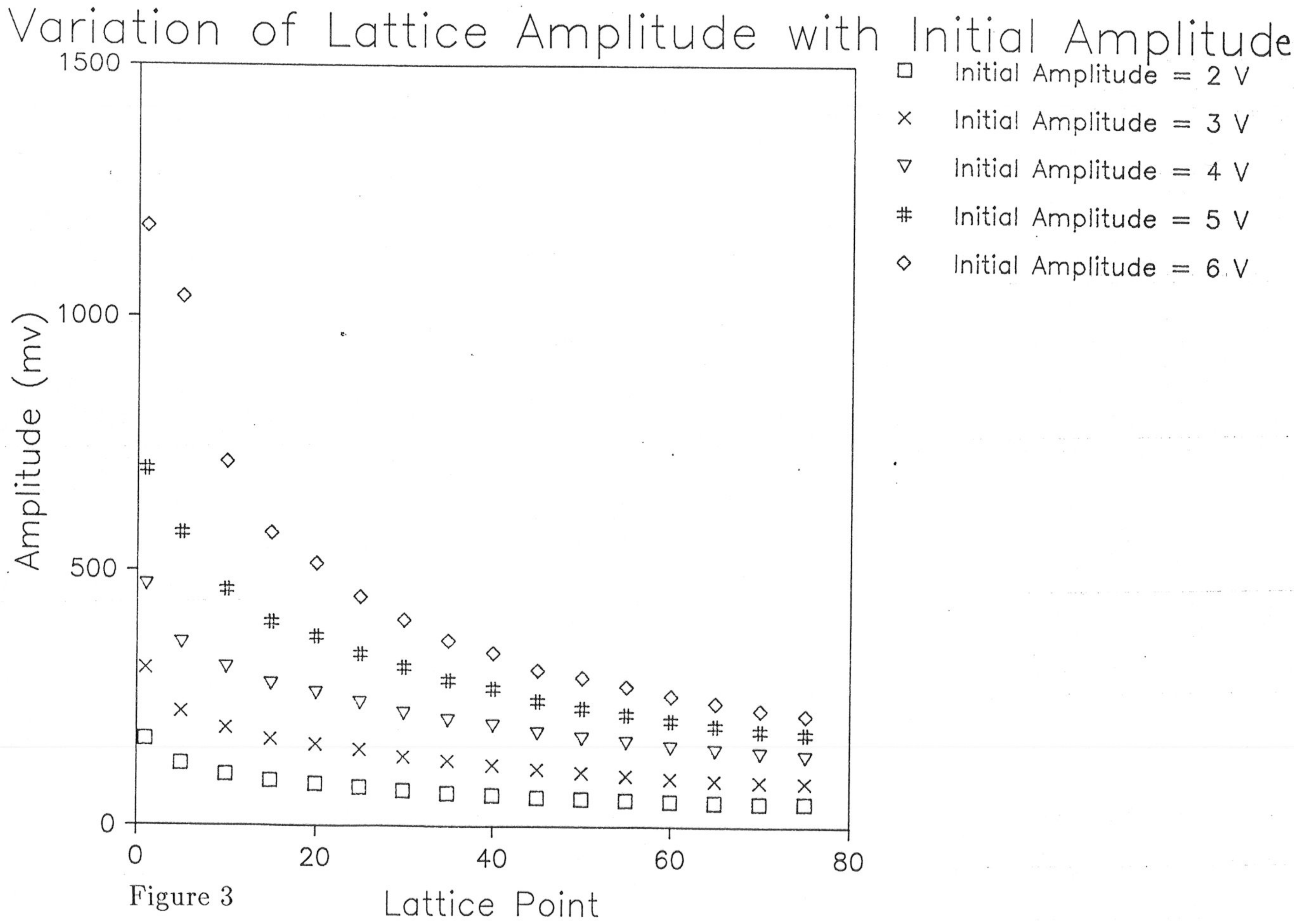

Variation of Lattice Amplitude with Initial Amplitude
Amplitude (mv)
1500
1000
500
0
0
20
40
60
80
Lattice Point
Initial Amplitude = 2 V
Initial Amplitude = 3 V
Initial Amplitude = 4 V
Initial Amplitude = 5 V
Initial Amplitude = 6 V

Figure 3

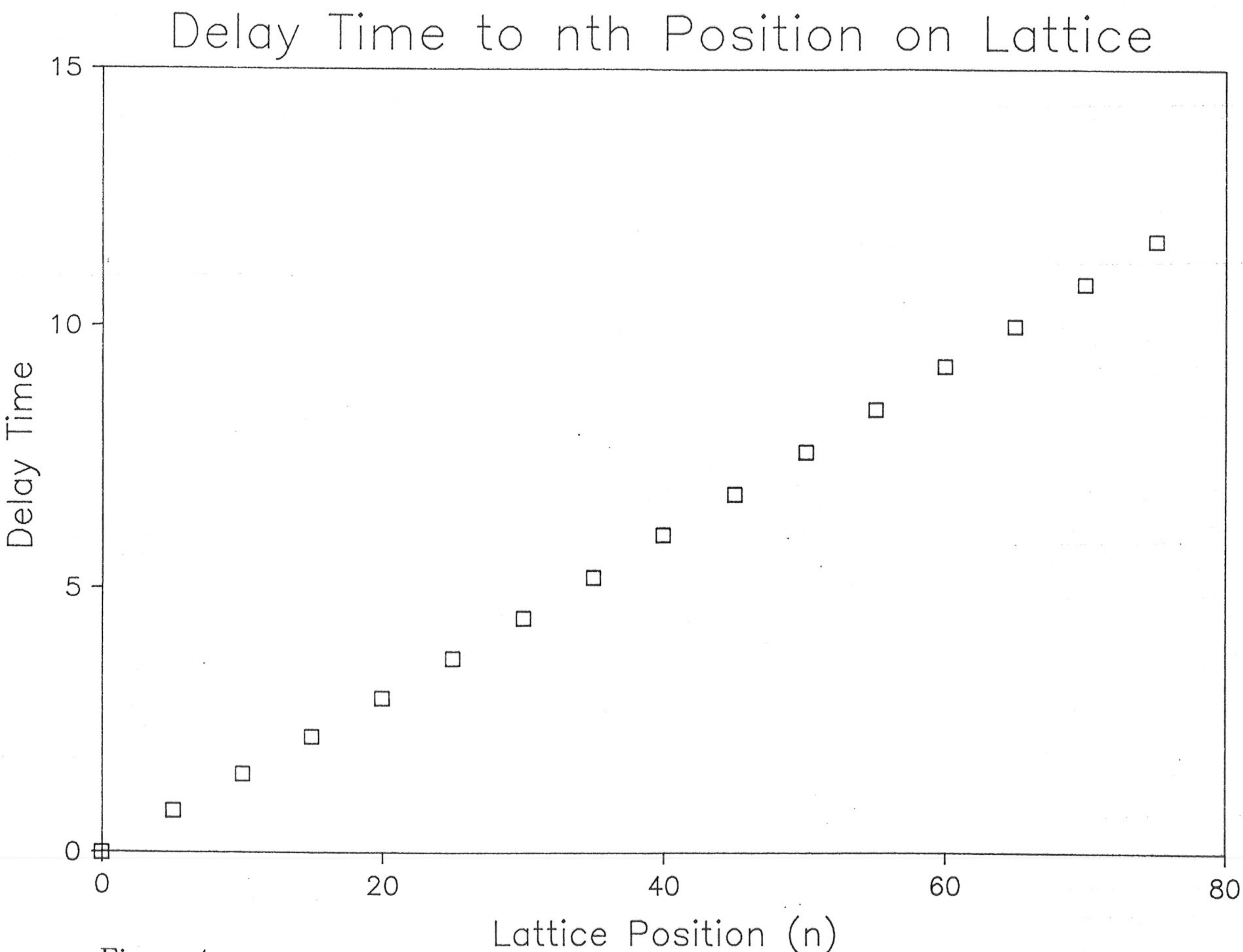
Delay Time to nth Position on Lattice
15
10
5
0
Delay Time
0
20
40
60
80
Lattice Position (n)

Figure 4

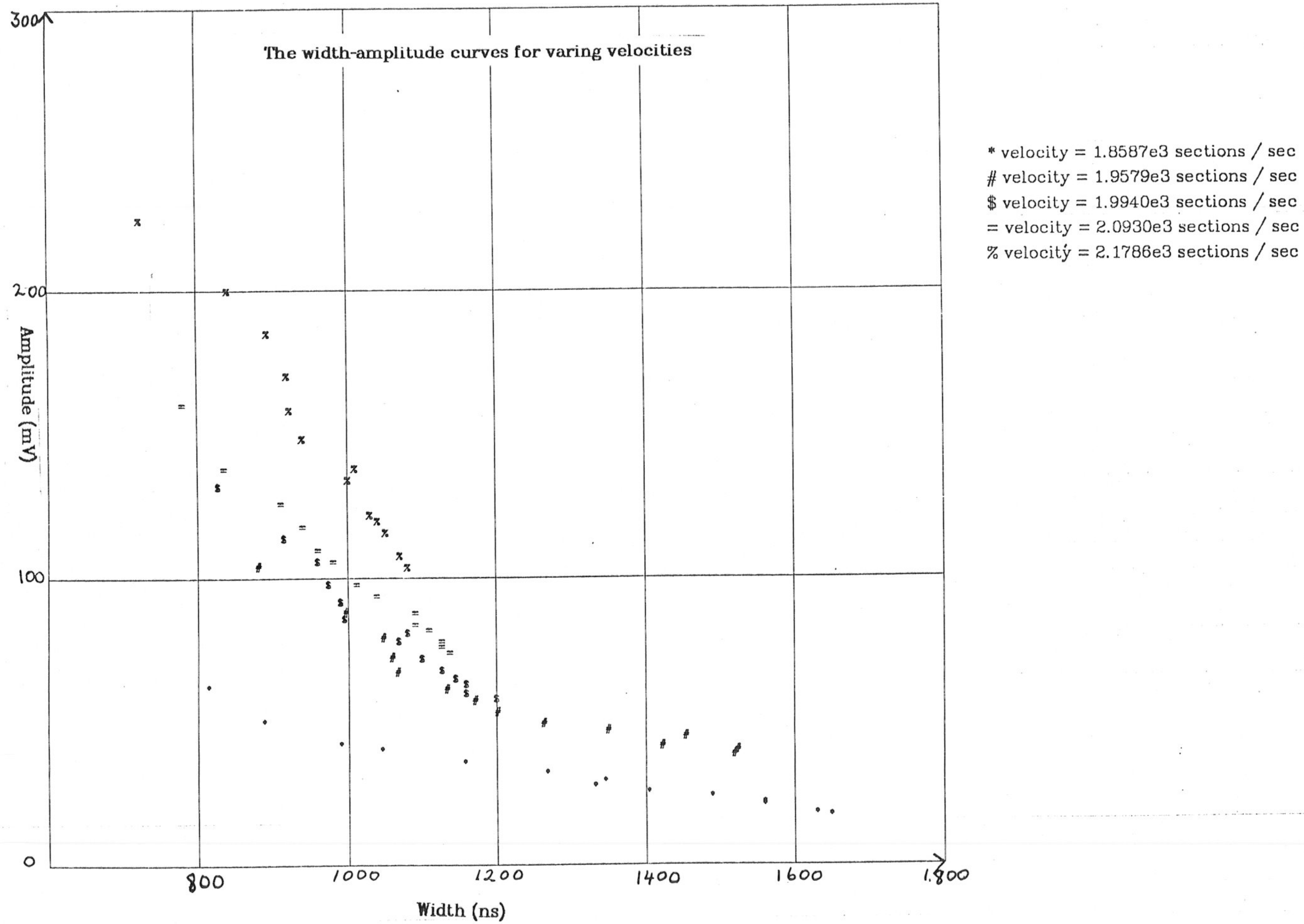
The width-amplitude curves for varing velocities
300
200
100
0
Amplitude (mV)
800
1000
1200
1400
1600
1800
Width (ns)
* velocity = 1.8587e3 sections / sec
# velocity = 1.9579e3 sections / sec
$ velocity = 1.9940e3 sections / sec
= velocity = 2.0930e3 sections / sec
% velocity = 2.1786e3 sections / sec

Figure 5

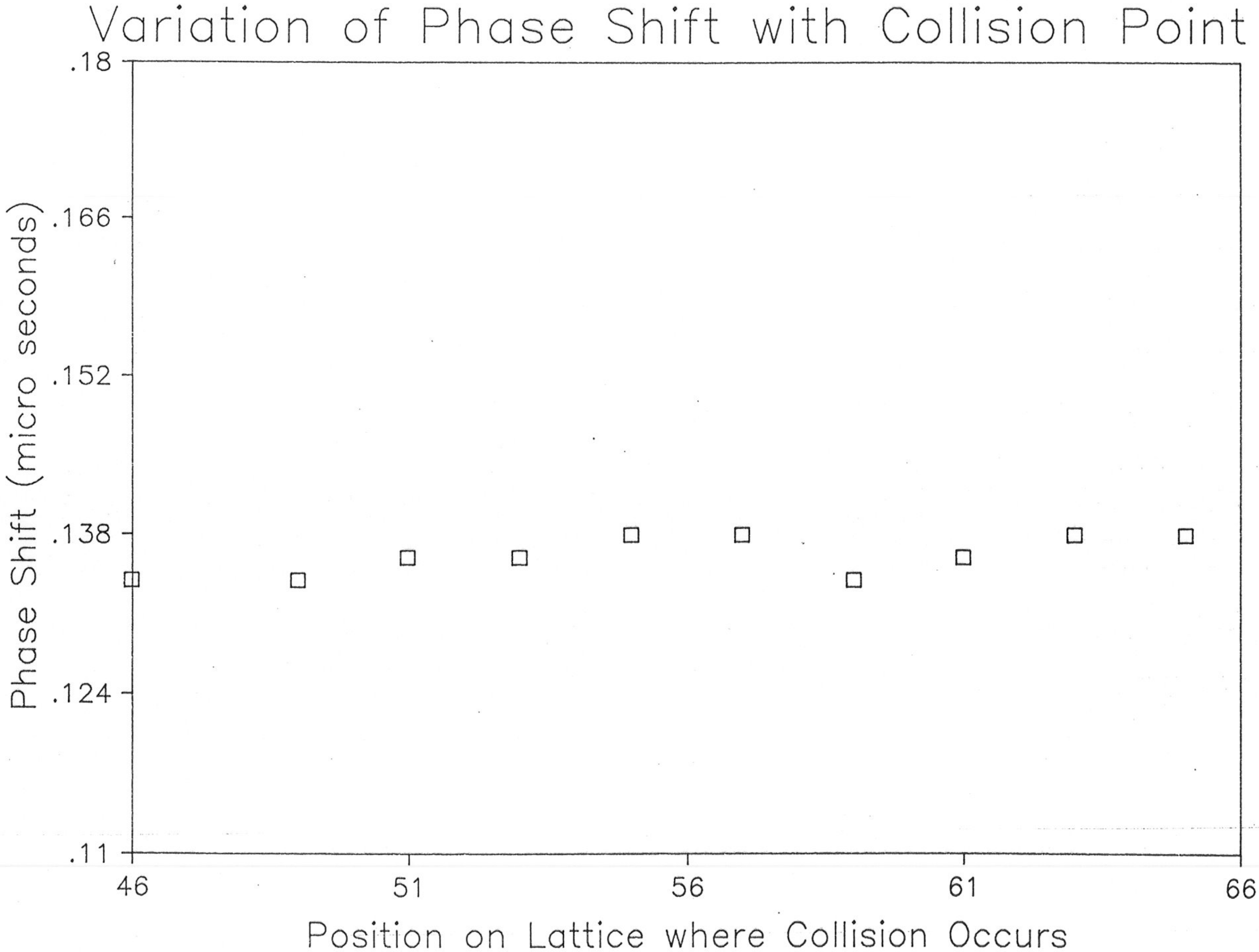
Variation of Phase Shift with Collision Point
Phase Shift (micro seconds)
.18
.166
.152
.138
.124
.11
46
51
56
61
66
Position on Lattice where Collision Occurs

Figure 6

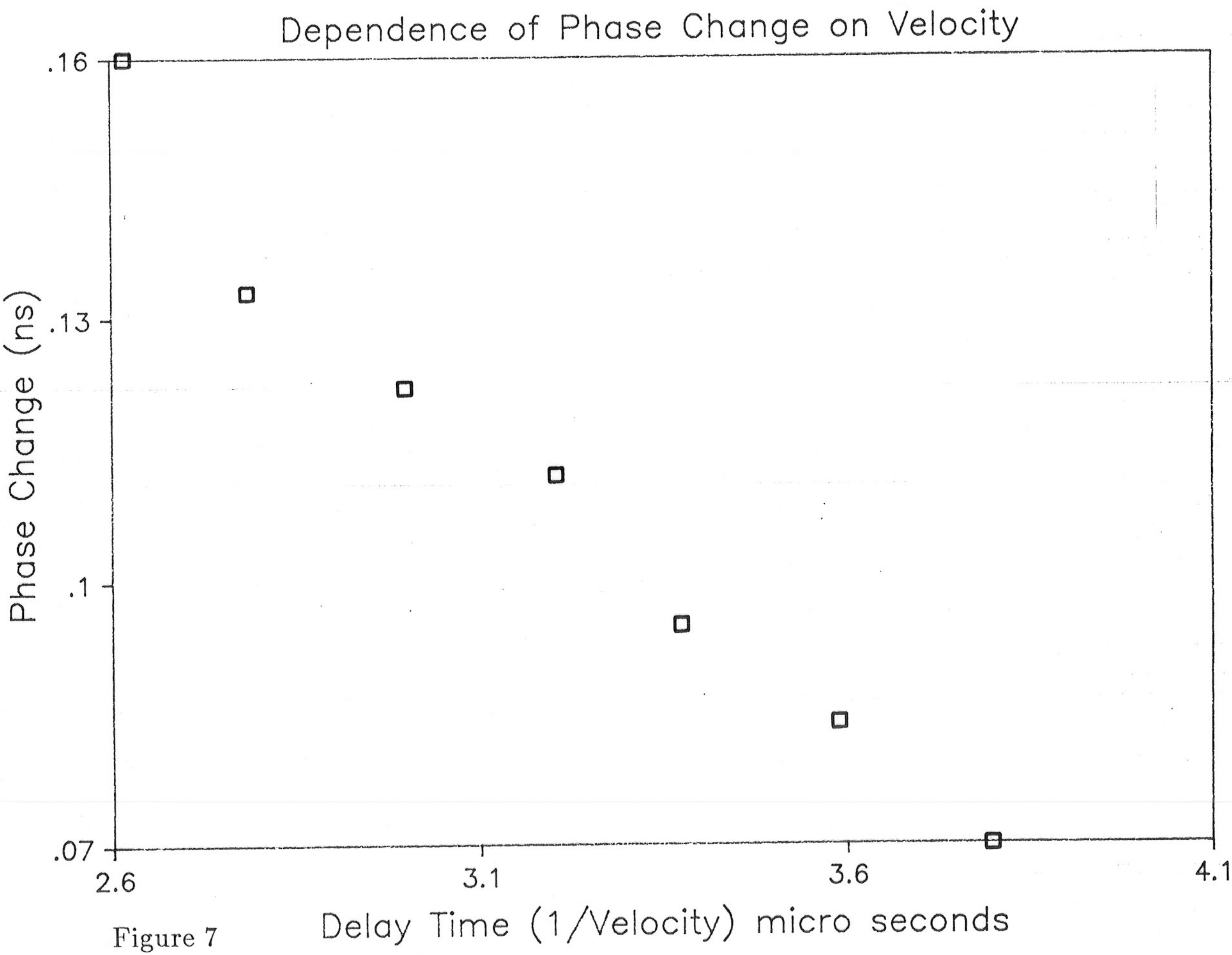
Dependence of Phase Change on Velocity
Phase Change (ns)
.16
.13
.1
.07
2.6
3.1
3.6
4.1
Delay Time (1/Velocity) micro seconds

Figure 7

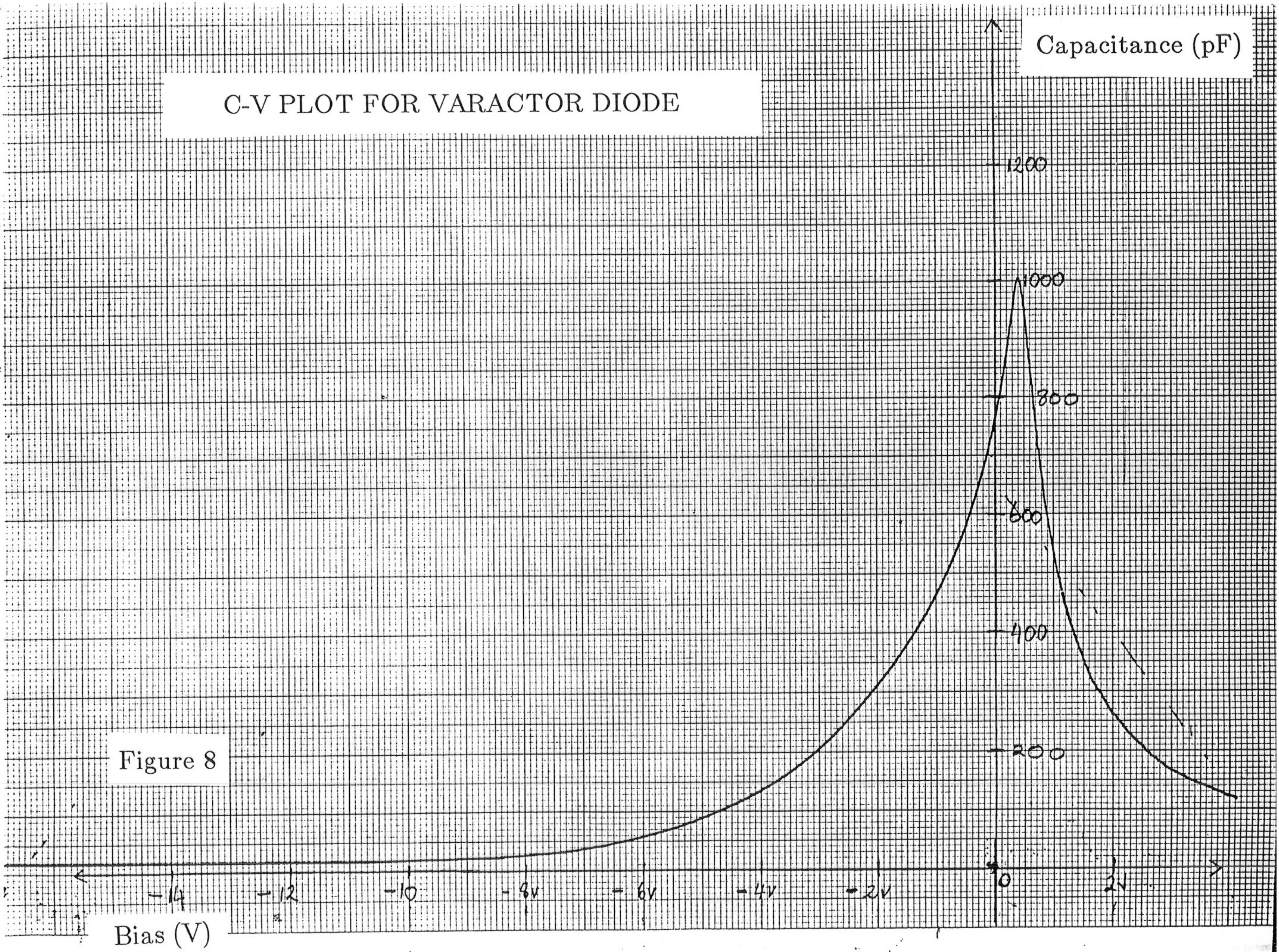
C-V PLOT FOR VARACTOR DIODE
Capacitance (pF)
Bias (V)
Figure 8